

# Minimum and Complete Fluidization Velocity for Sand-Palm Shell Mixtures, Part II: Characteristic Velocity Profiles, Critical Loading and Binary Correlations

V.S. Chok

Department of Chemical Engineering,  
Universiti Teknologi PETRONAS,  
31750 Tronoh, Perak, Malaysia  
chokvuisoon@yahoo.com.sg

A. Gorin, H.B. Chua

School of Engineering and Science,  
Curtin University of Technology Sarawak Campus,  
CDT 250, 98009 Miri, Sarawak, Malaysia  
alexander.g@curtin.edu.my

**Abstract**—In Part I of this work, the main features of the fluidization behavior and characteristic velocities as well as the utilization of these relationships to describe the fluidization mechanism and mixing/segregation tendency of sand-palm shell binary mixtures in compartmented fluidized bed gasifier (CFBG) have been reported. In the present work, the characteristic velocity profiles for various sand sizes, palm shell sizes and weight percents in the mixtures are presented. It is recognized that there are some instances where the mixtures characteristic values remain nearly unchanged from its pure sand values. This regime of constant values can be observed in both compartments, and can be established depending on the bed properties. The term “Critical loading” is then selected to define the maximum palm shell content (size and weight percent) that can be present in the sand where the mixtures characteristic velocities remain absolutely of pure sand values. The critical loading increases with the increase of sand size but decreases with the increase of palm shell size. Moreover, it can be observed that the critical loading generally decreases with the increase in particle size ratio, although exception is sighted in the combustor for the mixture with the largest sand size. This is due to the increased in particles mixing (described in Part I). Overall, the largest sand size has the highest critical loading in both compartments. Meanwhile, the selected correlations are able to describe the qualitative variation in the characteristic velocities of the mixtures. However, quantitatively, these correlations are unsatisfactory as they are either over-estimate or under-estimate.

**Keywords**-component; binary mixtures, biomass fluidization, compartmented fluidized bed; minimum fluidization velocity; complete fluidization velocity

## I. INTRODUCTION

Palm shell cannot be fluidized solely. It is considered as Geldart D particle, a classification for spouting material. However, the addition of a second fluidizable material (sand) in palm shell can facilitate proper fluidization. In Part I of this work [1], the main features of the fluidization behaviour and characteristic velocities using sand-palm shell mixtures were examined with respect to different bed properties. Their distinct patterns and further analysis on the various characteristic velocity relationships provide insights on the

fluidization mechanism and the mixing/segregation tendency. Some interesting works are given in [2]-[5] on hydrodynamic studies of sand-palm shell mixtures. Interested readers are encouraged to refer to them.

The present paper reports the characteristic velocity profiles for various sand sizes, palm shell sizes and weight percent in the mixtures and in different compartments. As described later, it is recognized that there are some instances where the mixtures  $U_{mf}$  and  $U_{cf}$  values remain nearly unchanged from its pure sand values. This regime of constant  $U_{mf}$  and  $U_{cf}$  values can be observed in both compartments, and can be established depending on the bed properties.

It is desirable to establish this regime for each compartment since the mixture characteristic velocities can be pre-determined using the bed material properties made up from entirely pure sand (inert) values. Within this regime, a single operational velocity can be set for the respective compartment based on the pure sand value and is independent from the variation of the palm shell size and weight percent in the mixtures (especially during combustion or gasification). Ultimately, the state of fluidization (e.g. bubbling or vigorously fluidized) and the condition of mixing/segregation in each compartment, that depend on the relative magnitude of the operational and characteristic velocities can be identified and maintained. Therefore, it is of great advantage to determine this regime for each compartment and the term “critical loading” is selected.

Meanwhile, various published  $U_{mf}$  and  $U_{cf}$  correlations are tested and compared with the experimental values.

## II. EXPERIMENTAL

### A. Apparatus

As the apparatus for this study is the same as described in [1], only a brief description is included here. A schematic of the experimental setup is illustrated in Fig. 1. The cold flow model as shown in Fig. 2 has a 0.66 ID and is divided into 2 compartments i.e. combustor and gasifier by a vertical wall in 2:1 cross-sectional area ratio. The effective diameters,  $D_e$  are

---

Authors would like to thank the Ministry of Science, Technology and Innovation and Malaysia Palm Oil Board for the financial support.

computed as 25.7 and 41.3 cm for gasifier and combustor respectively [1].

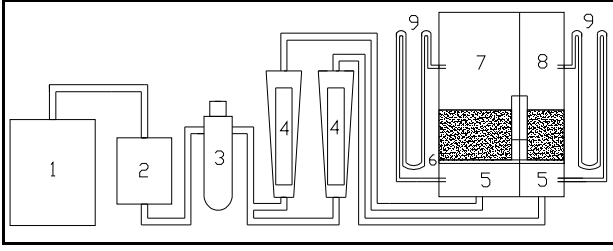


Figure 1. Experimental setup - 1: compressor; 2: dryer; 3: pressure regulator; 4: rotameter; 5: plenum; 6: perforated distributor; 7: combustor; 8: gasifier; 9: manometer [1]

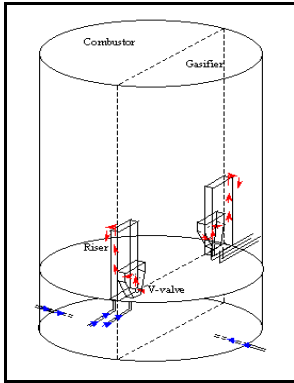


Figure 2. Isometric view of CFBG [1]

**B. Material**

The experiments were carried out in both of the compartments at 0.4 m static bed height. Large amount of bed material is used, i.e. at 77 and 101 kg respectively. 4 different types of sand and palm shell sizes are selected as the bed materials. The physical properties of the sand and palm shell are given in Table I.

TABLE I. PALM SHELL AND SAND PROPERTIES

Properties	Palm shell	Sand
Particle size/Sieved range (mm)	1.77/(+1.18-2.36)	0.196
	3.56/(+2.36-4.75)	0.272
	7.13/(+4.75-9.50)	0.341
	11.75/(+9.50-14.00)	0.395
Density (kg/m <sup>3</sup> )	1,500	2,700
Moisture (wt%)	8-10%	-
Weight Percent (wt%)	2, 5, 10, 15%	-

**III. RESULTS AND DISCUSSIONS**

**A. Characteristic Velocity Profiles**

Fig. 3 shows the  $U_{mf}$  and  $U_{cf}$  profiles in the combustor at various palm shell sizes and weight percent with finest sand of 196 $\mu$ m. For the smallest size palm shell of +1.18-2.36mm, both the  $U_{mf}$  and  $U_{cf}$  values remain unchanged from the values of pure sand as in [1]. Similarly, for medium size palm shell of +2.36-4.75mm, these values remain constant except at 15

wt%. With larger palm shell size of +4.75-9.50mm, the characteristic value changes at 5 to 10wt% but further increase of palm shell leads to severe channeling. This channeling condition is also observed for the largest palm shell size of +9.50-14.00mm where the characteristic velocities increase with the increase of palm shell wt% only up to 5wt%. Settlement of palm shell “chunks” are observed at higher weight percent for palm shell of > 4.75mm even at the maximum capacity of air flow rate (10 times  $U_{mf}$  of pure sand). Consequently, data that are not shown are due to poor fluidization.

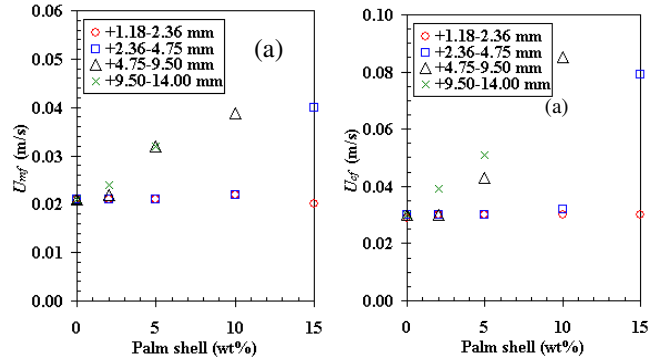


Figure 3.  $U_{mf}$  and  $U_{cf}$  in the combustor; sand of 196 $\mu$ m and palm shell of various sizes and weight percent

In addition, characteristic values for the sand-palm shell mixture in the gasifier are not presented here as channeling occurs even at smallest palm shell size and weight percent.

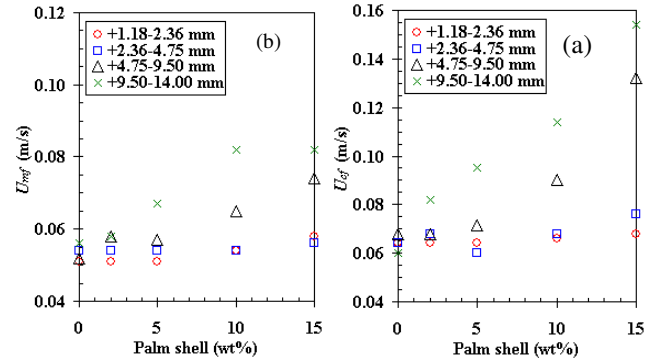


Figure 4.  $U_{mf}$  and  $U_{cf}$  in the combustor; sand of 272 $\mu$ m and palm shell of various sizes and weight percent

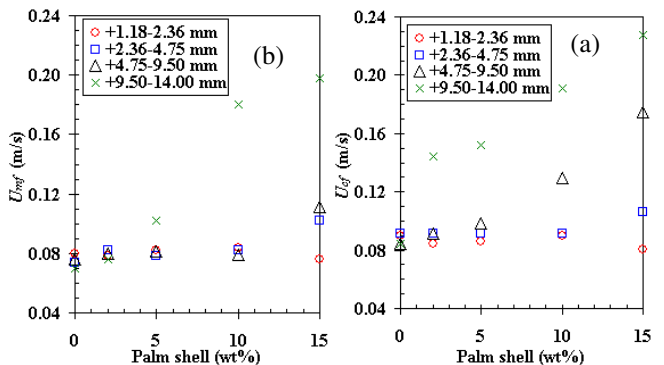


Figure 5.  $U_{mf}$  and  $U_{cf}$  in the gasifier; sand of 272 $\mu$ m and palm shell of various sizes and weight percent

Fig. 4(a) and 5(a) above indicate the  $U_{mf}$  values for gasifier and combustor at various palm shell sizes and wt% with river sand of 273 $\mu$ m.

The  $U_{mf}$  values remain unchanged in the combustor for palm shell size <4.75 mm. Although similarly is found in the gasifier, the  $U_{mf}$  increases at palm shell of +2.36-4.75mm at 15wt%. The  $U_{mf}$  increases at  $\geq 10$ wt% and  $\geq 5$ wt% for palm shell of +4.75-9.50mm and +9.50-14.00mm respectively in the combustor. However, in the gasifier, the effect of palm shell of +4.75-9.50mm and +9.50-14.00mm to the  $U_{mf}$  is noticeable at 15wt% and  $\geq 5$ wt% respectively.

The Fig. 4(b) and 5(b) above indicate the  $U_{cf}$  values for gasifier and combustor using the same river sand and palm shell composition. For palm shell size <4.75mm, the  $U_{cf}$  values in both compartments remain nearly unchanged except palm shell of +2.36-4.75mm at 15wt% in the gasifier. For palm shell size of +4.75-9.50mm,  $U_{cf}$  values for gasifier and combustor begin to show upward trends at  $\geq 10$ wt%.

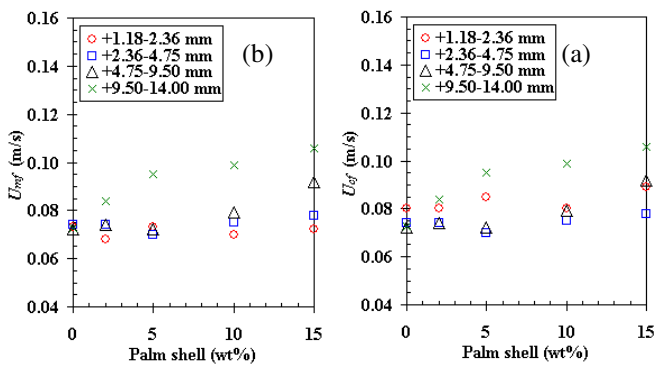


Figure 6.  $U_{mf}$  and  $U_{cf}$  in the combustor; sand of 341 $\mu$ m and palm shell of various sizes and weight percent

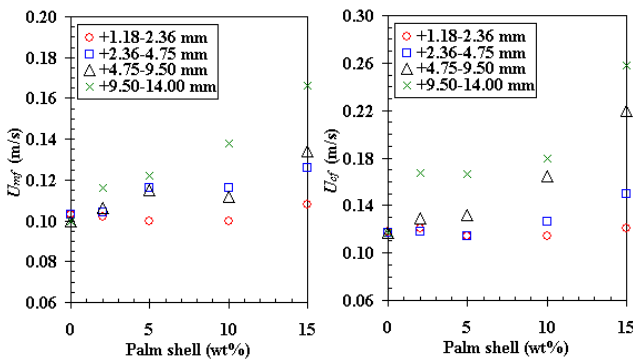


Figure 7.  $U_{mf}$  and  $U_{cf}$  in the gasifier; sand of 341 $\mu$ m and palm shell of various sizes and weight percent

Fig. 6(a) and 7(a) above indicate the  $U_{mf}$  values for combustor and gasifier at various palm shell sizes and wt% with larger sand of 341 $\mu$ m. No changes in the  $U_{mf}$  for palm shell size <9.50mm in the combustor, except for palm shell of +4.75 - 9.50mm at 15 wt%. This trend is also similarly observed in the gasifier, but with significant  $U_{mf}$  increase for palm shell of 2.36-4.75mm and +4.75-9.50mm at 15 wt%. In addition, for palm shell >9.50mm, at  $\geq 2$  wt%, increase of  $U_{mf}$  was observed in both compartments.

Fig. 6(b) and 7(b) above indicate the  $U_{cf}$  values for combustor and gasifier at various palm shell sizes and wt% with quartz sand of 341 $\mu$ m. No changes in the  $U_{cf}$  for palm shell size <4.75mm in the combustor. Similar trend is also obtained in the gasifier except a noticeable  $U_{cf}$  increase for palm shell of +2.36-4.75mm at 15 wt%. For palm shell of +4.75-9.50mm in the combustor, there is a marginal  $U_{cf}$  increase at 15wt%. A steep increase in  $U_{cf}$  is observed in the gasifier for palm shell of +4.75-9.50mm at  $\geq 10$  wt%. For palm shell of +9.50-14.00mm, incremental in  $U_{cf}$  values are observed at  $\geq 2$  wt%.

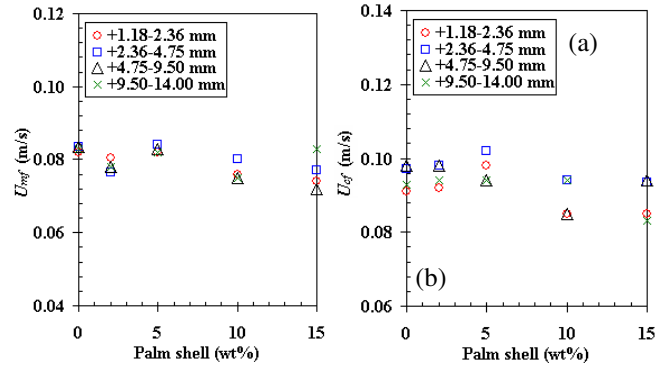


Figure 8.  $U_{mf}$  and  $U_{cf}$  in the combustor; sand of 395 $\mu$ m and palm shell of various sizes and weight percent

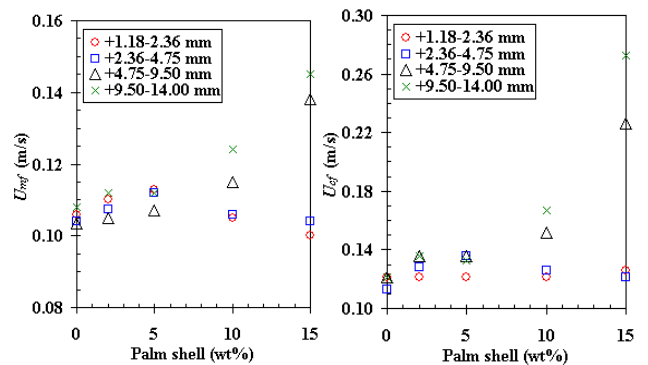


Figure 9.  $U_{mf}$  and  $U_{cf}$  in the gasifier; sand of 395 $\mu$ m and palm shell of various sizes and weight percent

Fig. 8 and 9 above indicate the  $U_{mf}$  and  $U_{cf}$  values for combustor and gasifier at various palm shell sizes and wt% with quartz sand of 395 $\mu$ m.

As shown in Fig. 8(a), the  $U_{mf}$  values in the combustor are relatively constant for all palm shell sizes at  $\leq 5$ wt%. However, slight decrease in the  $U_{mf}$  values are observed for palm shell sizes of  $\leq 9.50$ mm at  $\geq 10$ wt%. For the largest palm shell size of +9.50-14.00mm, the  $U_{mf}$  values remain unchanged. Similarly, in Fig. 8(b), the  $U_{cf}$  values in the combustor remain nearly unchanged for all palm shell sizes at  $\leq 5$ wt%. However, slight decrease in the  $U_{cf}$  values at 10wt% is noticeable for palm shell of +1.18-2.36mm and +4.75-9.50mm. For the largest palm shell size of +9.50-14.00mm, the  $U_{cf}$  values remain unchanged up to 10wt% and decreases at 15wt%.

In Fig. 9(a), the  $U_{mf}$  values for palm shell of  $\leq 4.75$ mm remains fairly constant up to 15wt% in the gasifier. However,

for palm shell size of  $\geq 4.75\text{mm}$ , at  $\geq 10\text{ wt}\%$ , increase of  $U_{mf}$  values are observed. Similarly found in Fig. 9(b), the  $U_{cf}$  values for palm shell of  $\leq 4.75\text{mm}$  remains constant in the gasifier. For palm shell size  $\geq 4.75\text{mm}$ , at  $\geq 10\text{ wt}\%$ , increase of  $U_{cf}$  was observed.

**B. Critical Loading**

Based on all the characteristic velocity profiles shown in Fig. 3-9, it is recognized that there are some instances where the mixtures  $U_{mf}$  and  $U_{cf}$  values remain nearly unchanged from its pure sand values. Therefore, it is of great advantage to determine this regime for each compartment and the term “critical loading” is selected. “Critical loading” is defined here as the maximum palm shell content (size and weight percent) that can be present in the sand where the mixtures  $U_{mf}$  and  $U_{cf}$  values remain absolutely of pure sand values. These values (of pure sand and mixture) are considered identical when the respective characteristic velocities variations between the bed materials are within  $\pm 15\%$ . Table II and III show the critical loading for  $U_{mf}$  and  $U_{cf}$  in the combustor and gasifier respectively.

TABLE II. CRITICAL LOADING FOR  $U_{mf}$  AND  $U_{cf}$  IN THE COMBUSTOR

Sand size ( $\mu\text{m}$ )	Palm shell size (mm)			
	+1.18-2.36	+2.36-4.75	+4.75-9.50	+9.50-14.00
	Palm shell weight percent (wt%); $U_{mf}/(U_{cf})$			
196	15/(15)	10/(5)	2/(2)	2/(0)
272	15/(15)	15/(10)	5/(5)	2/(0)
341	15/(15)	15/(10)	10/(5)	2/(2)
395	15/(15)	15/(15)	15/(15)	15/(10)

TABLE III. CRITICAL LOADING FOR  $U_{mf}$  AND  $U_{cf}$  IN THE GASIFIER

Sand size ( $\mu\text{m}$ )	Palm shell size (mm)			
	+1.18-2.36	+2.36-4.75	+4.75-9.50	+9.50-14.00
	Palm shell weight percent (wt%); $U_{mf}/(U_{cf})$			
196	-	-	-	-
272	15/(15)	10/(10)	10/(5)	2/(0)
341	15/(15)	10/(10)	10/(5)	2/(0)
395	15/(15)	15/(15)	10/(10)	5/(5)

In both Table II and III, it can be seen that for the smallest palm shell size of +1.18-2.36mm, up to 15 wt% can be present in the mixture with any sand sizes without resulting significant changes in the mixture characteristic velocities from the pure sand values.

In addition, the critical loading increases with the increase of sand size but decreases with the increase of palm shell size. Meanwhile, the critical loading for the  $U_{mf}$  is always equal or larger than the  $U_{cf}$  value in both of the compartments. Overall, the largest sand size (395 $\mu\text{m}$ ) has the highest critical loadings in both of the characteristic velocities.

Fig. 10 and 11 show the critical loading as a function of particle size ratio (palm shell/sand) in the combustor and gasifier respectively. The area below the lines and bounded by the horizontal axis represent the regime of the critical loading at various mixture size and composition. Generally, it can be observed that the critical loading decreases with the increase in particle size ratio i.e. in the trend of reducing. However, the formations of intermediate peaks occur in the combustor as

shown in Fig. 10 for the mixture with sand of 395 $\mu\text{m}$ . This is due to the increased in particles mixing as described earlier (Refer to Ratio of  $U_{cf}/U_{mf}$ ) as observed in the larger compartment. In addition, the critical loading line for the  $U_{mf}$  always lie on or above the values for the  $U_{cf}$ .

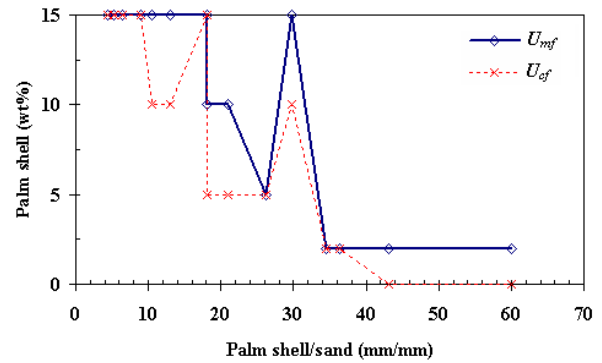


Figure 10. Critical loading in the combustor

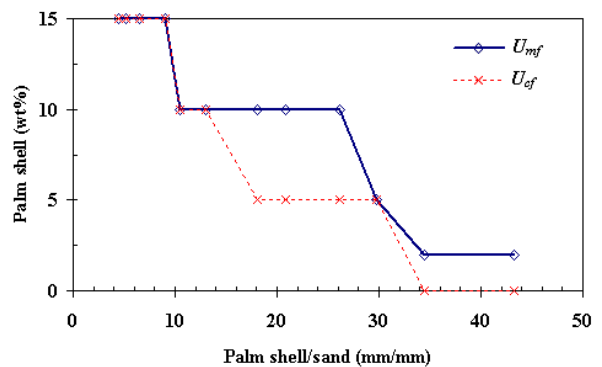


Figure 11. Critical loading in the gasifier

**C.  $U_{mf}$  and  $U_{cf}$  Values Comparison With Correlations**

The  $U_{mf}$  and  $U_{cf}$  values for sand/palm shell mixtures determined using the common methods for multi-components system allow comparative studies to be carried out from the various published correlations.

3 different binary correlations namely Mourad *et al.* [6], Goosens *et al.* [7] and Thonglimp *et al.* [8] are selected for comparison with experimental  $U_{mf}$  values. In addition, 4 different binary correlations namely Noda *et al.* [9], Mourad *et al.* [6], Gauthier *et al.* [10] and Rao *et al.* [11] are selected for comparison with experimental  $U_{cf}$  values. These researchers also utilized similar bed material properties and/or Geldart classification. The characteristic values for mixtures within the critical loading are not included since the mixtures  $U_{mf}$  and  $U_{cf}$  remain unchanged from the pure sand values.

In Fig. 12, it can be seen that all the  $U_{mf}$  correlations generally are able to describe the qualitative variation in the sand-palm shell binary mixtures, i.e. the correlations are able to show the increasing or decreasing trends with respect to different sand-palm shell composition. However, as shown in Fig. 13, quantitatively, most correlations are unsatisfactory as they are either over-estimate or under-estimate these values.

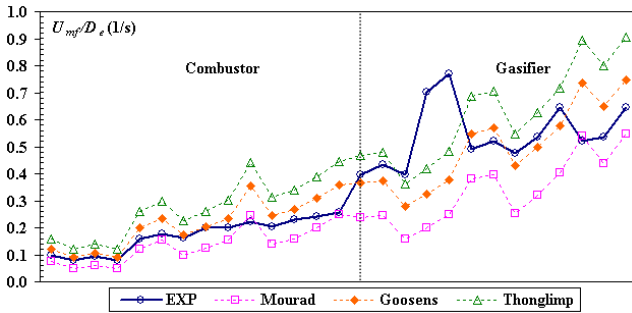


Figure 12: Comparison of experimental (EXP)  $U_{mf}/D_e$  with correlations; Mourad *et al.*[6], Goossens *et al.*[7], Thonglimp *et al.*[8]

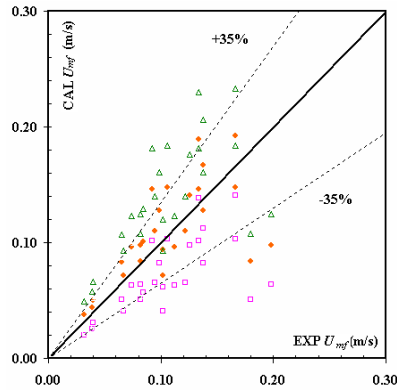


Figure 13: Comparison of experimental (EXP)  $U_{mf}$  with correlations; Mourad *et al.*[6], Goossens *et al.* [7] and Thonglimp *et al.*[8]

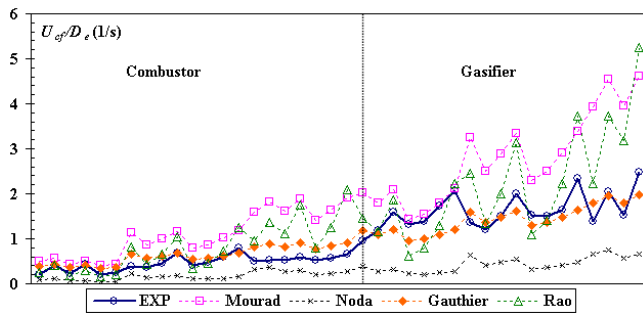


Figure 14: Comparison of experimental (EXP)  $U_{cf}/D_e$  with correlations; Mourad *et al.*[6], Noda *et al.*[9], Gauthier *et al.*[10] and Rao *et al.*[11]

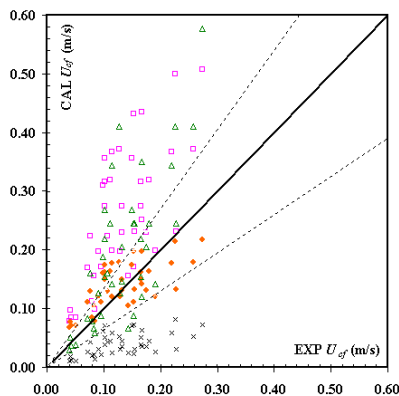


Figure 15: Comparison of experimental (EXP)  $U_{cf}$  with correlations; Mourad *et al.*[6], Noda *et al.*[9], Gauthier *et al.*[10] and Rao *et al.*[11]

Similar found in Fig. 14 and 15, all the  $U_{cf}$  correlations generally shows the qualitative  $U_{cf}$  variation for the sand-palm shell binary mixtures but unable to give satisfactory prediction. The results from the various comparisons made on the existing  $U_{mf}$  and  $U_{cf}$  correlations at different palm shell and sand mixtures clearly show that significant deviation exceeding  $\pm 35\%$  from experimental values.

#### IV. CONCLUSION

Taking into account all of the  $U_{mf}$  and  $U_{cf}$  values at different palm shell and sand mixtures and fitting all these curves to a single mathematical equation is seemingly impractical. Although for a specific palm shell size and sand,  $U_{mf}$  and  $U_{cf}$  can be fitted into an equation but no correct equation and model which can correlate all of the data that have been found thus far. Direct utilizing of the experimental values for the operation of sand-palm shell in fluidized bed is essential. Alternatively, identifying the critical loading for this mixture provides a convenient yet robust system where its operational velocity can be pre-determined using bed material properties made up from entirely pure sand (inert) values.

#### REFERENCES

- [1] V.S. Chok, S.K. Wee, A. Gorin and H.B. Chua, "Effect of particle and bed diameter on characteristic velocities in Compartmented Fluidized Bed Gasifier," 2<sup>nd</sup> CUTSE International Conference: Progress in Science and Engineering for Sustainable Development, 24-25<sup>th</sup> November 2009, unpublished.
- [2] V.S. Chok, A. Gorin and H.B. Chua, "Minimum and Complete Fluidization Velocity for Sand/Palm Shell Binary Mixtures, Part I: Fluidization Behaviour and Characteristic Velocities," 2<sup>nd</sup> CUTSE International Conference: Progress in Science and Engineering for Sustainable Development, 24-25<sup>th</sup> November 2009, unpublished.
- [3] V.S. Chok, L.F.B. Chin, S.K. Wee, W.W. Tang, A. Gorin, H.B. Chua and H.M. Yan, "Hydrodynamics studies of sand/palm shells binary mixtures in compartmented fluidized bed gasifier (CFBG)," 1<sup>st</sup> Engineering Conference on Energy & Environment (EnCon), UNIMAS, Kuching, Sarawak, December 2007.
- [4] M. Fauziah, A.R. Norazah and A. Nornizar, "Fluidization of palm oil residues in binary particle system," 21<sup>st</sup> Symposium of Malaysia Chemical Engineers (SOMChE), Universiti Teknologi MARA, 2006.
- [5] M. Fauziah, A.R. Nornizar, A. Nornizar, A. Azil Bahari and M.J. Tajuddin, "Cold flow binary fluidization of oil palm residues mixture in a gas-solid fluidized bed system," *Pertanika Journal of Science and Technologi*, 2008, vol. 16(2), pp. 201-212.
- [6] M. Mourad, M. Hemati and C. Laguerie, "Hydrodynamiques d'un sechir a lit fluidise a flottation: Determination des vitesses caracteristiques de fluidisation de melanges de maïs et de sable," *Powder Technology*, 1994, vol. 80, pp. 45-54.
- [7] W.R.A. Goossens, G.L. Dumont, G.J. Spaepen, "Fluidization of binary mixtures in the laminar flow reaction," *Chemical Engineering Program Symposium Series*, 1971, vol. 67(116), pp. 38-45.
- [8] V. Thonglimp, N. Hiquily and C. Laguerie, "Vitesse minimale de fluidisation et expansion des couches de melanges de particulates solides fluidisees par un gaz," *Powder Technology*, 1984, vol. 39, pp. 223-239.
- [9] K. Noda, S. Uchida, T. Makino, H. Kamo, "Minimum fluidization velocity of binary mixtures of particles with large size ratio," *Powder Technology*, vol. 46, 1986, pp. 149 - 154.
- [10] D. Gauthier, S. Zerguerras and G. Flamant, "Influence of the particle size distribution of powders on the velocities of minimum and complete fluidization," *Chemical Engineering Journal*, 1999, vol. 74, pp. 181-196.
- [11] T.R. Rao, J.V. Ram. Bheemarasetti, "Minimum fluidization velocity of mixtures of biomass and sands," *Energy*, vol. 26, 2001, pp. 633 - 644.